

# Observing the helium abundance with CMB

Roberto Trotta<sup>1,\*</sup> and Steen H. Hansen<sup>2,†</sup>

<sup>1</sup>*Département de Physique Théorique, Université de Genève,  
24 quai Ernest Ansermet, CH-1211 Genève 4, Switzerland*

<sup>2</sup>*Physik Institut, Winterthurerstrasse 190, 8057 Zurich, Switzerland*

We consider for the first time the ability of present-day cosmic microwave background (CMB) anisotropies data to determine the primordial helium mass fraction,  $Y_p$ . We find that CMB data alone gives the confidence interval  $0.160 < Y_p < 0.501$  (at 68% c.l.). We analyse the impact on the baryon abundance as measured by CMB and discuss the implications for big bang nucleosynthesis. We identify and discuss correlations between the helium mass fraction and both the redshift of reionization and the spectral index. We forecast the precision of future CMB observations, and find that Planck alone will measure  $Y_p$  with error-bars of 5%. We point out that the uncertainty in the determination of the helium fraction will have to be taken into account in order to correctly estimate the baryon density from Planck-quality CMB data.

## I. INTRODUCTION

Our understanding of the baryon abundance has increased dramatically over the last few years. This improvement comes from two independent paths, namely big bang nucleosynthesis (BBN) and cosmic microwave background radiation (CMB). Absorption features from high-redshift quasars allow to measure precisely the deuterium abundance, D/H. Combined with BBN calculations, this provides a reliable estimate of the baryon to photon ratio,  $\eta$ . An independent determination of the baryon content of the universe from CMB anisotropies comes from the increasingly precise measurements of the acoustic peaks, which bear a characteristic signature of the photon-baryon fluid oscillations. The agreement between these two completely different approaches is both remarkable and impressive (see details below). The time is therefore ripe to proceed and test the agreement between other light elements which are also probed both with BBN and CMB.

The helium abundance has been measured for many years from astrophysical systems. However, the error-bars are seemingly dominated by systematic errors which are hard to assess. Fortunately, the dependence of the helium mass fraction on the CMB anisotropies provides an independent way to measure  $Y_p$ . The aim of this work is to present the first determination of the helium abundance from CMB alone, and to clarify the future potential of this method. The latest CMB data are precise enough to allow taking this further step, and in view of the emerging “baryon tension” between BBN predictions from observations of different light elements [1] possibly requires taking such a step. The advantage of using CMB anisotropies rather than the traditional astrophysical measurements, is that CMB provide a clear measurement of the primordial helium fraction before it could be changed by any astrophysical process. On the other

hand the dependence of the CMB power spectrum on  $Y_p$  is rather mild, a fact which makes it presently safe to set the helium mass fraction to a constant for the purpose of CMB data analysis of other cosmological parameters.

The paper is organized as follows. In section II we review the standard Big Bang Nucleosynthesis scenario. Section III discusses the role of the helium mass fraction for cosmic microwave background anisotropies, the methods used and results. We discuss our forecast for future CMB observations in section III D, and offer our conclusions in section IV

## II. BIG BANG NUCLEOSYNTHESIS

### A. The standard scenario

The standard model of big bang nucleosynthesis (SBBN) has only one free parameter, namely the baryon to photon ratio  $\eta_{10} = n_b/n_\gamma 10^{10}$ , which for long has been known to be in the range  $1 - 10$  [2]. Thus by observing just one primordial light element one can predict the abundances of all the other light elements.

The deuterium to hydrogen abundance, D/H, is observed by Ly- $\alpha$  features in several quasar absorption systems at high red-shift,  $D/H = 2.78_{-0.38}^{+0.44} \times 10^{-5}$  [3], which in SBBN translates into the baryon abundance,  $\eta_{10} = 5.9 \pm 0.5$ . Using SBBN one thus predicts the helium mass fraction to be in the range  $0.2470 < Y_p < 0.2487$ . The dispersion in various deuterium observations is, however, still rather large, ranging from  $D/H = 1.65 \pm 0.35 \times 10^{-5}$  [4] to  $D/H = 3.98_{-0.67}^{+0.59} \times 10^{-5}$  [3], which most probably indicates underestimated systematic errors.

The observed helium mass fraction comes from the study of extragalactic HII regions in blue compact galaxies. One careful study [5] gives the value  $Y_p = 0.244 \pm 0.002$ ; however, also here there is a large scatter in the various observed values, ranging from  $Y_p = 0.230 \pm 0.003$  [6] over  $Y_p = 0.2384 \pm 0.0025$  [7] and  $Y_p = 0.2391 \pm 0.0020$  [8] to  $Y_p = 0.2452 \pm 0.0015$  [9]. Besides the large scatter there is also the problem that

\*Electronic address: roberto.trotta@physics.unige.ch

†Electronic address: hansen@physik.unizh.ch

the helium mass fraction predicted from observation of deuterium combined with SBBN,  $0.2470 < Y_p < 0.2487$ , is larger than (and seems almost in disagreement with) most of the observed helium abundances, which probably points towards underestimated systematic errors, rather than the need for new physics [1, 10]. Figure 1 is a compilation of the above measurements, and offers a direct comparison with the current (large) errors from CMB observations (presented in section III below) and with the potential of future CMB measurements (discussed in section III D).

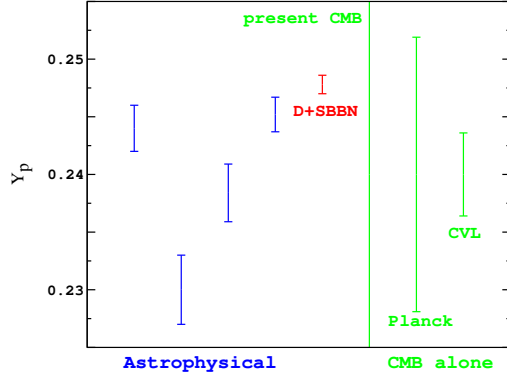


FIG. 1: On the left (blue) we plot a few current direct astrophysical measurements of the helium mass fraction  $Y_p$  with their  $1 - \sigma$  statistical errors, and the value inferred from deuterium measurements combined with SBBN (red) (see text for references). On the right (green), a direct comparison with CMB present-day accuracy (actual data, this work; the errorbar extends in the range  $0.16 < Y_p < 0.50$ ) and with its future potential (Fisher matrix forecast for Planck and a Cosmic Variance Limited experiment).

The observed abundance of primordial  $^7\text{Li}$  using the Spite plateau is possibly spoiled by various systematic effects [11, 12]. Therefore it is more appropriate to use the SBBN predictions together with observations to estimate the depletion factor  $f_7 = {^7\text{Li}_{\text{obs}}}/{^7\text{Li}_{\text{prim}}}$  instead of using  $^7\text{Li}_{\text{obs}}$  to infer the value of  $\eta$  [13, 14].

The numerical predictions of standard BBN (as well as various non-standard scenarios) have reached a high level of accuracy [13, 15, 16, 17], and the precision of these codes is well beyond the systematic errors discussed above.

## B. The role of neutrinos

If the CMB-determined helium mass fraction turns out to be as high as suggested by SBBN calculations together with the CMB observation of  $\Omega_b h^2$  (as discussed above), this could indicate a systematic error in the present direct astrophysical helium observations. Alternatively, if the CMB could independently determine the helium value with sufficient precision to confirm the present helium

observations, then this would be a smoking gun for new physics. In fact, one could easily imagine non-standard BBN scenarios which would agree with present observations of  $\eta_{10}$ , while having a low helium mass fraction. All that is needed is additional non-equilibrium electron neutrinos produced at the time of neutrino decoupling which would alter the  $n - p$  reaction. This could alter the resulting helium mass fraction while leaving the deuterium abundance unchanged. One such possibility would be a heavy sterile neutrino whose decay products include  $\nu_e$ . A sterile neutrino with life-time of  $1 - 5$  sec and with decay channel  $\nu_s \rightarrow \nu_e + \phi$  with  $\phi$  a light scalar (like a majoron), would leave the deuterium abundance roughly untouched, but can change the helium mass fraction between  $\Delta Y_p = -0.025$  and  $\Delta Y_p = 0.015$  if the sterile neutrino mass is in the range  $1 - 20$  MeV [18]. A simpler model would be standard neutrino oscillation between a sterile neutrino and the electron neutrino. The lifetime is about 1 sec when the sterile state has mass about 10 MeV, and the decay channel is  $\nu_s \rightarrow \nu_e + l + \bar{l}$  (with  $l$  any light lepton), and such masses and life-times are still unconstrained for large mixing angle [19] (related BBN issues are discussed in refs. [20, 21, 22]). Such possibilities are hard to constrain without an independent measurement of the helium mass fraction.

Another much studied effect of neutrinos is the increased expansion rate of the universe if additional degrees of freedom are present (for BBN), and the degeneracy between the total density in matter and relativistic particles (for CMB). This issue has recently been studied in detail in refs. [10, 23] in view of the new WMAP results, and we need not discuss this further here. Also an electron neutrino chemical potential could potentially alter the BBN predictions [24], however, with the observed neutrino oscillation parameters the different neutrino chemical potentials would equilibrate before the onset of BBN [25], hence virtually excluding this possibility (see however [26]).

## III. COSMIC MICROWAVE BACKGROUND

### A. Photon recombination and reionization

The recent WMAP data allow one to determine with very high precision the epoch of photon decoupling,  $z_{\text{dec}}$ , *i.e.* the epoch at which the ionized electron fraction,  $x_e(z) = n_e/n_H$ , has dropped from 1 to its residual value of order  $10^{-4}$ . Here  $n_e$  denotes the number density of free electrons, while  $n_H$  is the total number density of H atoms (both ionized and recombined). After this moment, photons are no longer coupled to electrons (last scattering), and they free stream. The redshift of decoupling has been determined to be  $z_{\text{dec}} = 1088^{+1}_{-2}$  [27], which corresponds to a temperature of about 0.25 eV. Helium recombines earlier than hydrogen, roughly in two steps: around redshift  $z = 6000$  HeIII recombines to HeII, while HeII to HeI recombination begins around

$z < 2500$  and finishes just after the start of H recombination (see e.g. [28, 29, 30, 31]).

Denoting by  $n_{He}$  and  $n_b$  the number densities of He atoms and baryons, respectively, the helium mass fraction is defined as  $Y_p = 4n_{He}/n_b$ . The baryon number density is related to the baryon energy density today,  $\omega_b$ , by  $n_b = 11.3(1+z)^3\omega_b$  and we have  $n_H = n_b(1-Y_p)$ . Usually, the ionization history is described in terms of  $x_e(z) = n_e/(n_b(1-Y_p))$ . However, for the purpose of discussing the role of  $Y_p$ , it is more convenient to consider the quantity  $f_e(z) = n_e/n_b$  instead, the ratio of free electrons to the total number of baryons. For brevity, we will call  $f_e$  the free electron fraction. Once the baryon number density has been set by fixing  $\omega_b$ , one can think of  $Y_p$  as an additional parameter which controls the number of free electrons available in the tight coupling regime. The CMB power spectrum depends on the full detailed evolution of the free electron fraction, but we can qualitatively describe the role of helium in four different phases of the ionization/recombination history (see Fig. 2).

- (a) Before HeIII recombination all electrons are free, therefore  $f_e(z > 6000) = 1 - Y_p/2$ .
- (b) HeII progressively recombines and just before H recombination begins,  $f_e$  has dropped to the value  $f_e(z \approx 1100) = 1 - Y_p$ .
- (c) After decoupling, a residual fraction of free electrons freezes out, giving  $f_e(30 \lesssim z \lesssim 800) = f_e^{\text{res}} \approx 2.7 \cdot 10^{-5} \sqrt{\omega_m}/\omega_b$ .
- (d) Reionization of all the H atoms gives  $f_e(z \lesssim 20) = 1 - Y_p$ .

During phase (a), the photon-baryons fluid is in the tight coupling regime. However the presence of ionized He increases diffusion damping, therefore having an impact on the damping scale in the acoustic peaks region. When the detailed energy levels structure of HeII is taken into account [31], the transition to phase (b) is smoother than in the Saha equation approximation. Therefore the plateau with  $f_e = 1 - Y_p$  is not visible in Fig. 2. Before H recombination, He atoms remain tightly coupled to H atoms through collisions, with the same dynamical behaviour. In particular, it is the total  $\omega_b$  which determines the amount of gravitational pressure on the photon-baryons fluid, and which sets the acoustic peak enhancement/suppression. Hence we do not expect the value of  $Y_p$  to have any influence on the boosting (suppression) of odd (even) peaks. The redshift of decoupling (transition between (b) and (c)) depends mildly on  $Y_p$  in a correlated way with  $\omega_b$ , since the number density of free electrons in the tight coupling regime (just before H recombination) scales as  $n_e = f_e n_b = n_b(1 - Y_p)$ . Hence an increase in  $\omega_b$  can be compensated by allowing for a larger helium fraction. An analytical estimate along the same lines as in e.g. [2] indicates that a 10% change in  $Y_p$  affects  $z_{\text{dec}}$  by roughly 0.1%, which corresponds to

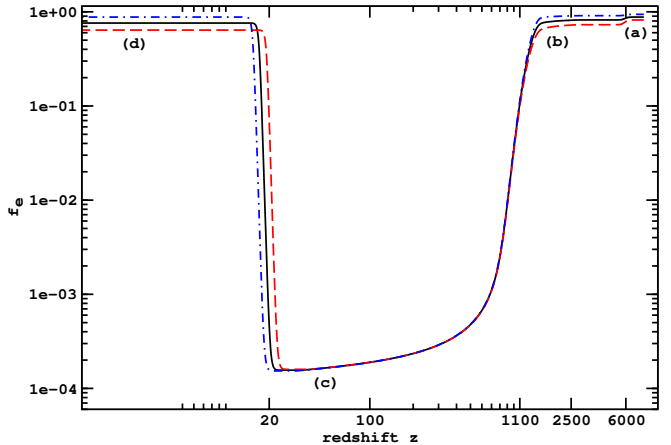


FIG. 2: Evolution of the number density of electrons normalized to the number density of baryons,  $f_e = n_e/n_b$ , as a function of redshift for different values of the helium fraction  $Y_p$ . The black-solid curve corresponds to the standard value  $Y_p = 0.24$ , the red-dashed (blue-dot-dashed) to  $Y_p = 0.36$  ( $Y_p = 0.12$ ). The labels (a) to (d) indicate the four different phases discussed in the text.

$\Delta z_{\text{dec}} \approx 1$ . This is of the same order as the current  $1-\sigma$  errors on  $z_{\text{dec}}$ , obtained by fixing  $Y_p = 0.24$ .

After H recombination, the residual ionized electron fraction  $f_e^{\text{res}}$  does not depend on  $Y_p$ , but is inversely proportional to the total baryon density (phase (c)). As the CMB photons propagate, they are occasionally scattered by the residual free electrons. The corresponding optical depth,  $\tau^{\text{res}}$  is given by

$$\begin{aligned} \tau^{\text{res}} &= \int_{t_0}^{t_{\text{dec}}} n_e^{\text{res}} c \sigma_T dt \\ &\approx 1.86 \cdot 10^{-6} \sqrt{\Omega_m} \int_0^{z_{\text{dec}}} \frac{(1+z)^2}{(\Omega_m(1+z)^3 + \Omega_\Lambda)^{1/2}} dz. \end{aligned} \quad (1)$$

Neglecting the contribution of the cosmological constant at small redshift, the integral can be performed and the approximated optical depth from the residual ionization fraction is estimated to be

$$\tau^{\text{res}} \approx 1.24 \cdot 10^{-6} (1 + z_{\text{dec}})^{3/2} \approx 0.045, \quad (2)$$

independent of the cosmological parameters and of the helium fraction. Therefore after last scattering we do not expect any significant effect on CMB anisotropies coming from the primordial helium fraction, until the reionization epoch.

Fairly little is known about the exact reionization mechanism and its redshift dependence (for a review see e.g. [32]). Observation of Gunn-Peterson troughs indicate

that the universe was completely ionized after redshift  $z \approx 6$ , when the universe seemingly completed the reionization [33], possibly for the second time [34]. Since CMB anisotropies are sensitive only to the integrated reionized fraction (and lacking a more precise model) we assume that at the reionization redshift  $z_r$  all the hydrogen was quickly reionized, thus producing a sharp rise of  $n_e$  from its residual value to  $n_H$ . More precisely,  $z_r$  is the redshift at which  $x_e(z_r) = 0.5$ . In our treatment we neglect HeII reionization, for which there is evidence at a redshift  $z \approx 3$  (see [35] and references therein). This effect is small, since the extra electron released at  $z \approx 3$  would change the reionization optical depth by about only 1%. We also neglect the increase of  $Y_p$  due to non-primordial helium production, which has an negligible effect on CMB anisotropies. Those approximations do not affect the results at today's level of sensitivity of CMB data, however, a more refined modelling of the reionization mechanism is needed in order to correctly analyse Planck-quality data. The relation between reionization redshift and reionization optical depth,  $\tau_r$ , is given by

$$\begin{aligned} \tau_r &= \int_{t_0}^{t_{\text{reion}}} n_e c \sigma_T dt \\ &\approx 11.3 c \sigma_T \omega_b (1 - Y_p) \int_0^{z_r} \frac{d\eta}{da} dz, \end{aligned} \quad (3)$$

where  $t$  is physical time,  $\eta$  is conformal time and  $a$  the scale factor. Here again, since the number density of reionized electrons scales as  $\omega_b(1 - Y_p)$ , the redshift of reionization is positively correlated with  $Y_p$  (for fixed optical depth and baryon density).

As a result of the physical mechanism described above, a 10% change in  $Y_p$  has a net impact on the CMB power spectrum at the percent level. The impact on the CMB temperature and polarization power spectra is highlighted in Fig. 3. In the temperature panel, we notice that a larger helium fraction slightly suppresses the peaks because of diffusion damping, while it has no impact on large scales. Polarization is induced by the temperature quadrupole component at last scattering. When reionization occurs, there is a generation of polarized power on the scale corresponding to the acoustic horizon size at the reionization redshift. This particular signature is called the 'reionization bump', and is clearly visible in the bottom panel of Fig. 3 in the  $\ell \approx 10$  region. As discussed above, a change in the helium fraction implies a shift of the redshift of reionization for a given (fixed) optical depth, and therefore a sideways shift of the reionization bump in the polarization power spectrum. This is shown in the bottom panel: a 10% change in  $Y_p$  induces roughly a 10% change in the position of the bump (the subsequent two oscillatory features for  $\ell \lesssim 50$  are numerical artifacts which arise because polarization goes almost to 0 in that region). It is therefore clear that a good determination of the reionization bump will assist in determining the helium abundance accurately.

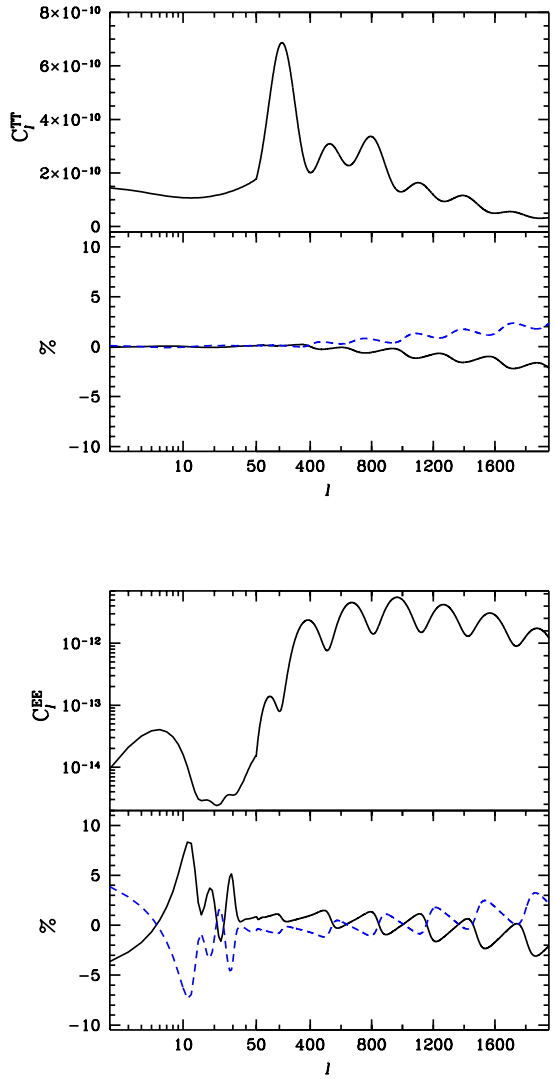


FIG. 3: CMB temperature (top panel) and polarization (bottom panel) power spectra and percentage difference with two different values of the helium fraction for a standard  $\Lambda$ CDM model. The solid-black (dashed-blue) line corresponds to a 10% larger (smaller) value of  $Y_p$  wrt to the standard value,  $Y_p = 0.24$ . All other parameters are fixed to the value of our fiducial model (Table I), in particular, we have  $\tau_r = 0.166$ .

## B. Monte Carlo analysis

We use a modified version of the publicly available Markov Chain Monte Carlo package COSMOMC [36] as described in [37] in order to construct Markov Chains in our 7 dimensional parameter space. We sample over the following set of cosmological parameters: the physical baryon and CDM densities,  $\omega_b \equiv \Omega_b h^2$  and  $\omega_c \equiv \Omega_c h^2$ , the cosmological constant in units of the critical density,  $\Omega_\Lambda$ , the scalar spectral index and the overall normal-

ization of the power spectrum,  $n_s$  and  $A_s$  (see section III D below for a more precise definition), the redshift at which the reionization fraction is a half,  $z_r$ , and the primordial helium mass fraction,  $Y_p$ . We restrict our analysis to flat models, therefore the Hubble parameter,  $h = H_0/100 \text{ km s}^{-1}\text{Mpc}^{-1}$ , is a derived parameter,  $h = [(\omega_c + \omega_b)/(1 - \Omega_\Lambda)]^{1/2}$ . We consider purely adiabatic initial conditions, and we do not include gravitational waves. In the CMB analysis, we assume 3 massless neutrino families and no massive neutrinos. We include the WMAP data [38, 39] (temperature and polarization) with the routine for computing the likelihood supplied by the WMAP team [40]. We make use of the CBI [41] and of the decorrelated ACBAR [42, 43] band powers above  $\ell = 800$  to cover the small angular scale region of the power spectrum.

Since  $Y_p$  is a rather flat direction in parameter space with present-day data, we find that a much larger number of samples is needed in order to achieve good mixing and convergence of the chains in the full 7D space. We use  $M = 4$  chains, each containing approximately  $N = 3 \cdot 10^5$  samples. The mixing diagnostic is done on the same lines as in [40], by means of the Gelman and Rubin criterion [44]. The burn-in of the chains also takes longer than in the case where  $Y_p$  is held fixed, and we discard 6000 samples per chain.

### C. CMB analysis results

Marginalizing over all other parameters, we find that the helium mass fraction from CMB alone is constrained to be  $Y_p < 0.647$  at 99% c.l. (1 tail limit), and

$$0.160 < Y_p < 0.501 \quad (4)$$

at 68% c.l. (2 tails). Thus, for the first time the primordial helium mass fraction has been observed using the cosmic microwave background. However, present-day CMB data do not have sufficient resolution to discriminate between the astrophysical helium measurements,  $Y_p \sim 0.244$ , and the deuterium guided BBN predictions,  $Y_p \sim 0.248$ , which would require percent precision.

In Figure 4 we plot the marginalized and the mean likelihood of the Monte Carlo samples as a function of  $Y_p$ . If the likelihood distribution is Gaussian, then the 2 curves should be indistinguishable. The difference between marginalized and mean likelihood for  $Y_p$  indicates that the marginalized parameters are skewing the distribution, and therefore that correlations play an important role. Although the mean of the 1D marginalized likelihood is rather high,  $\langle \mathcal{L}(Y_p) \rangle = 0.33$ , the mean likelihood peaks in the region indicated by astrophysical measurements,  $Y_p \sim 0.25$ . In view of this difference, it is important to understand the role of correlations with other parameters, and we will turn to this issue now.

In Figure 5 we plot joint 68% and 99% confidence contours in the  $(\omega_b, Y_p)$ -space. From the Monte Carlo samples we obtain a small and negative correlation coeffi-

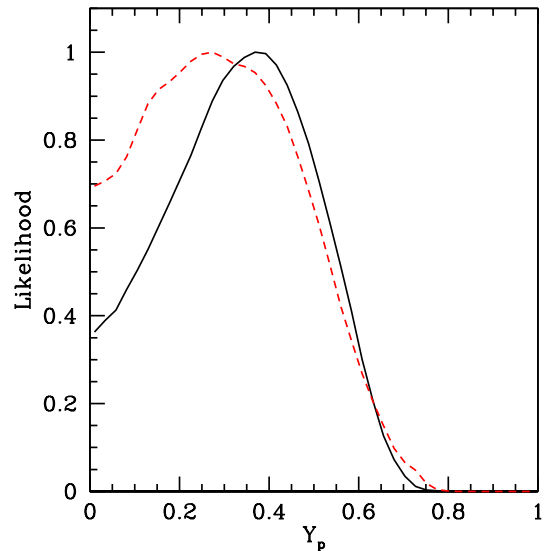


FIG. 4: One-dimensional posterior likelihood distribution for the helium mass fraction,  $Y_p$ , using CMB data only. The solid-black line is for all other parameters marginalized, the dashed-red line gives the mean likelihood.

cient between the two parameters  $\text{corr}(Y_p, \omega_b) = -0.14$ . Baryons and helium appear to be anticorrelated simply because present-day WMAP data do not map the peaks structure to sufficiently high  $\ell$ . Precise measurements in the small angular scale region should reveal the expected positive correlation between the baryon and helium abundances, which is potentially important in order to correctly combine BBN predictions and CMB measurements of the baryon abundance. We turn to this question in more detail in the next section. In SBBN the baryon fraction and helium fraction are correlated along a different direction (cf. Fig. 5). However, this correlation is very weak, and the SBBN relation gives practically a flat line. Since the two parameters are not independent from the CMB point of view, it is in fact not completely accurate to do the CMB analysis with fixed helium mass fraction of  $Y_p = 0.24$  to get the error-bars on the baryon fraction, and then re-input this baryon fraction (and error-bars) to predict the helium mass fraction from BBN. The most accurate procedure is to analyse the CMB data leaving  $Y_p$  as a free parameter, thereby obtaining the correct (potentially larger) error-bars on  $\omega_b$  upon marginalization over  $Y_p$ .

In view of the emerging baryon tension between CMB and BBN, it is important to check whether allowing helium as a free parameter can significantly change the CMB determination of the baryon density or its error. In order to evaluate in detail the impact of  $Y_p$  on the error-bars for  $\omega_b$ , we consider the following 3 cases.

- (a) The usual case, when the helium fraction for the CMB analysis is assumed to be known *a priori* and

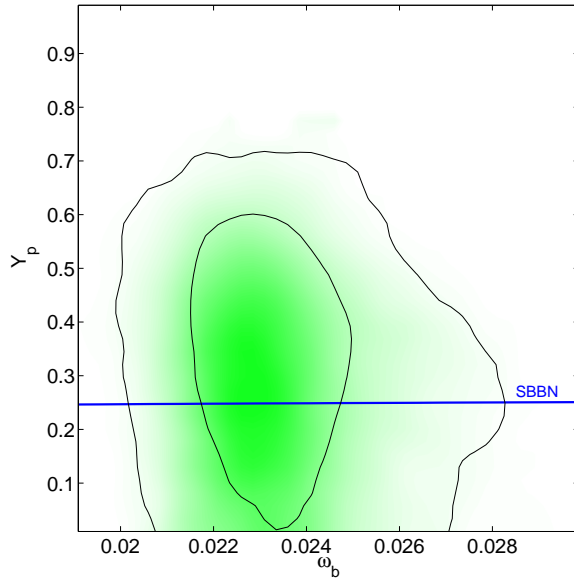


FIG. 5: Joint 68% and 99% confidence contours in the  $(\omega_b, Y_p)$ -plane from CMB data alone. The solid-blue line gives the SBBN prediction [13], which on this figure almost looks like a straight line.

is fixed to the canonical value  $Y_p = 0.24$ .

- (b) A case with a weak astrophysical Gaussian prior on the helium fraction, which we take to be  $Y_p = 0.24 \pm 0.01$ . As discussed above, the error-bars of the astrophysical measurements are typically a factor 5 tighter than this, but our prior is chosen to encompass the systematic spread between the different observations.
- (c) The case in which we do not assume any prior for  $Y_p$  and we let it vary as a totally free parameter.

We do not find any significant change in the error-bars for  $\omega_b$  in the 3 different cases. The confidence intervals on  $\omega_b$  alone are determined to be (case (c))  $0.0221 < \omega_b < 0.0245$  at 68% c.l. ( $0.0204 < \omega_b < 0.0276$  at 99 % c.l.). The standard deviation of  $\omega_b$  as estimated from the Monte Carlo samples is found to be  $\hat{\sigma}_b = 1.3 \cdot 10^{-3}$ . This is in complete agreement with the error-bars on  $\omega_b$  obtained by the WMAP team for the standard  $\Lambda$ CDM case [27]. We conclude that at the level of precision of present-day CMB data, it is still safe to treat the baryon abundance and the helium mass fraction as independent parameters. However, the  $Y_p - \omega_b$  correlation will have to be taken into account to correctly analyse future CMB data, with a quality such as Planck. We discuss this potential in the next section. Other light elements like deuterium and helium-3 are much less abundant, and will therefore have even smaller effect on the CMB power spectrum, at the order of  $10^{-5}$ .

We observe the expected correlation between the redshift of reionization and the helium fraction (Fig. 6),

which is discussed above. The correlation coefficient between the two parameters is found to be rather large and positive,  $\text{corr}(Y_p, z_r) = 0.40$ . This correlation produces a noticeable change in the marginalized 1D-likelihood distribution for  $z_r$  as we go from case (a) to case (c). Marginalization over the additional degree of freedom given by  $Y_p$  broadens considerably the error-bars on  $z_r$ . In fact, the 68% confidence interval for  $z_r$  increases by roughly 20% (and shifts to somewhat higher values), from  $10.2 - 20.9$  (case (a)) to  $10.6 - 23.3$  (case (c)). Case (b) exhibits similar error-bars as case (a). On the other hand, the determination of the reionization optical depth is not affected by the inclusion of helium as a free parameter, giving in all cases  $0.08 < \tau_r < 0.23$ . Correspondingly, the correlation is less significant,  $\text{corr}(Y_p, \tau_r) = -0.11$ . We therefore conclude that the differences in the determination of  $z_r$  are due only to the variation of the amount of electrons available for reionization as  $Y_p$  is changed.

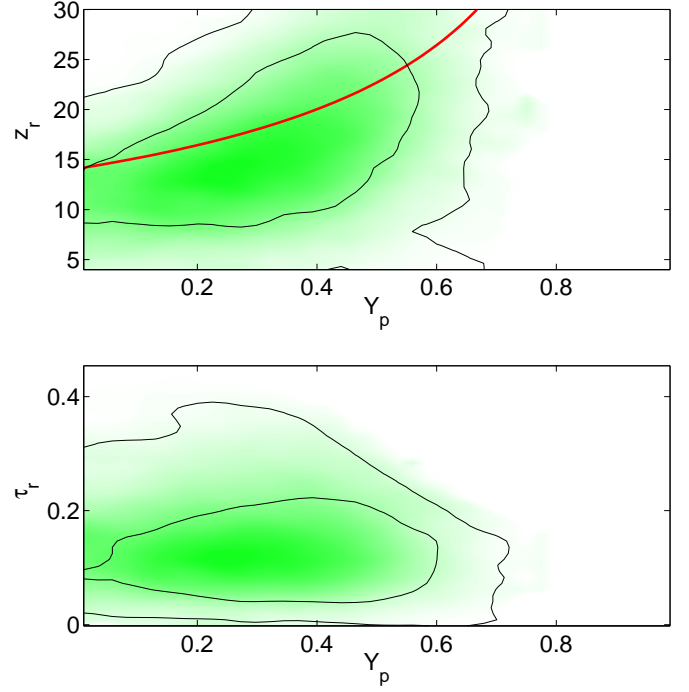


FIG. 6: Joint 68% and 99% confidence contours in the  $(Y_p, z_r)$ -plane (upper panel) and in the corresponding  $(Y_p, \tau_r)$ -plane (bottom panel) from CMB data alone. In the upper panel, the solid-red line is the relation  $z_r(Y_p)$  from eq. (3), obtained by fixing the reionization optical depth to the value  $\tau_r = 0.166$ , while the other parameters are the ones of our fiducial  $\Lambda$ CDM model. Although clearly the exact shape of  $z_r(Y_p)$  depends on the particular choice of cosmology, it is apparent that the  $Y_p - z_r$  degeneracy is along this direction. The correlation between  $Y_p - \tau_r$  is almost negligible with present-day data (bottom panel).

Leaving  $Y_p$  as a free parameter also has an impact on the relation between  $\omega_b$  and the scalar spectral index,  $n_s$ . The extra power suppression on small scales which

is produced by a larger  $Y_p$  can be compensated by a blue spectral index (see Fig. 7).

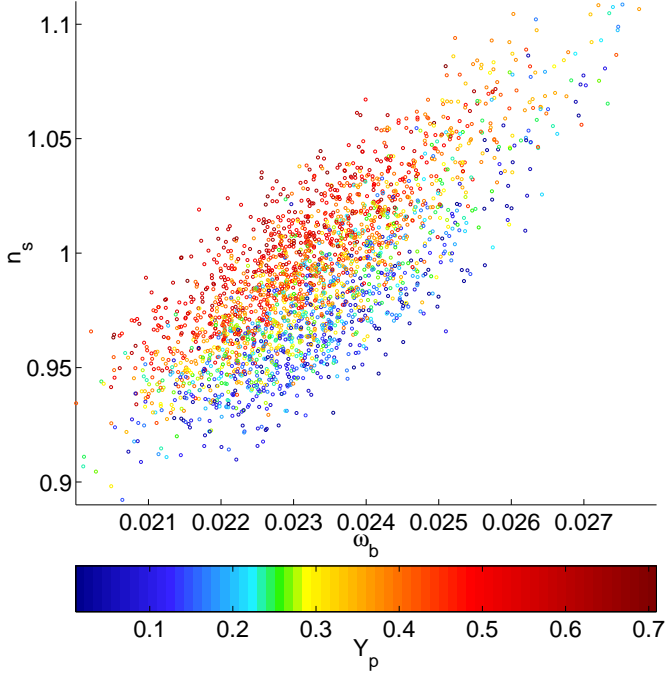


FIG. 7: Scatter plot in the  $\omega_b - n_s$  plane, with the value of  $Y_p$  rendered following the colour scale. Green corresponds roughly to the SBBN preferred value.

#### D. Potential of future CMB observations

In order to estimate the precision with which future satellite CMB measurements will be able to constrain the helium mass fraction we perform a Fisher matrix analysis (FMA). This technique approximates the likelihood function with a Gaussian distribution around a fiducial model, which is assumed to be the best fit model. The Fisher information matrix  $F$  gives the second order expansion of the likelihood around its peak, and it is computed from the derivatives of the power spectrum with respect to the cosmological parameters. The expected performance of the experiment can be modelled with a noise contribution to the likelihood function, which is described in terms of a few experimental parameters. The covariance matrix  $C$  is then given by the inverse of the Fisher matrix,  $C = F^{-1}$ . It is then straightforward to evaluate the expected  $1-\sigma$  error on parameter  $i$ , which is given by  $\sqrt{c_{ii}}$  (all other marginalized). The main advantage of the FMA is that it gives reliable and accurate predictions (including information on the expected degeneracies) with minimal computational effort. For further details on the Fisher Matrix formalism, see e.g. [45, 46, 47, 48, 49, 50, 51, 52].

#### 1. Parameters set

In order to obtain a reliable prediction, it is extremely important to choose a parameter set wrt which the dependence of the CMB power spectrum is as linear and uncorrelated as possible. This issue has been discussed exhaustively in Ref. [53], where the authors introduce a set of “physical parameters” which satisfies the above requirements. In the present work we retain most of the physical parameters defined in ref. [53]: the ratio between the sound horizon at decoupling and the angular diameter distance  $\mathcal{A}$ , the baryon density  $\mathcal{B} = \Omega_b h^2$ , the energy density in the cosmological constant  $\mathcal{V} = \Omega_\Lambda h^2$ , the matter-radiation density at decoupling  $\mathcal{R}$  and  $\mathcal{M}$ , which is mainly a function of the matter and radiation content. We adopt a slightly different choice for the physical parameter describing reionization. For adiabatic perturbations, the initial power spectrum of the gauge invariant curvature perturbation  $\zeta$  is written as

$$P_\zeta(k) = A_s \left( \frac{k}{k_0} \right)^{n_s - 1}$$

(and we do not take running into account). The quantity  $\zeta$  corresponds to the intrinsic curvature perturbation on comoving hypersurfaces, and at the end of inflation is related to the gravitational potential perturbation,  $\Psi$ , by  $\zeta = \frac{3}{2}\Psi$  (see e.g. [54] for more details). We take the pivot-scale  $k_0$  to be  $k_0 = 0.05 \text{ Mpc}^{-1}$ . If  $\tau_r$  denotes the optical depth to reionization, then defining  $\mathcal{T} = A_s \exp(-2\tau_r)$  is a good way to take into account the degeneracy between the optical depth and normalization. Our parameter set contains then the six above physical parameters  $(\mathcal{A}, \mathcal{B}, \mathcal{V}, \mathcal{R}, \mathcal{M}, \mathcal{T})$ , the power spectrum normalization  $A_s$ , the scalar spectral index  $n_s$  and the helium fraction  $Y_p$ .

The choice of the physical parameter set makes it easy to implement in the FMA interesting theoretical priors. For instance, we are interested in imposing flatness in our forecast, in order to be able to directly compare present-day accuracy on  $Y_p$  with the potential of Planck and CVL. The prior on the curvature of the universe is imposed in the FMA by fixing the value of the parameter  $\mathcal{A}$  to the one of the fiducial model. In fact, the parameter  $\mathcal{A}$  is a generalization of the shift parameter, which describes the sideway shift of the acoustic peak structure of the CMB power spectrum as a function of the geometry of the universe and its content in matter, radiation and cosmological constant. Although imposing  $\mathcal{A} = \text{const}$  is not the same as having curvature=constant over the full range of cosmological parameters, for the purpose of evaluating derivatives the two conditions reduce to the same. The fact that our fiducial model is actually slightly open (see below), does not make any substantial difference in the results, apart from reducing the numerical inaccuracies which would arise had we computed the derivatives around an exactly flat model. We can also easily impose a prior knowledge of the helium fraction, by fixing the

value of  $Y_p$ , as it is usually done in present CMB analysis, and investigate how this modifies the expected error on the baryon density.

## 2. Accuracy issues

We numerically compute double sided derivative of the power spectrum around the fiducial model with cosmological parameters given in Table I. We find it necessary to increase the accuracy of CAMB by a factor of 3 in each of the “accuracy boost” values. As a fiducial model, we use the best fit model to the WMAP data for the standard  $\Lambda$ CDM scenario, as given in Table 1 of ref. [27]. However, in order to avoid numerical inaccuracies which arise when differentiating around a flat model, we reduce slightly the value of  $\Omega_\Lambda$  by imposing an open universe,  $\Omega_{\text{tot}} = 0.99$ . We perform the FMA for the expected capabilities of Planck’s High Frequency Instrument (HFI) and for an ideal CMB measurement which would be cosmic variance limited (CVL) both in temperature and in E-polarization (and we do not consider the B-polarization spectrum), and therefore represents the best possible parameter measurement from CMB anisotropies alone. The complicated issues coming from foreground removals, point source subtractions, etc. are assumed to be already (roughly) taken into account in the experimental parameters for the experiment. Those are the effective percentual sky coverage  $f_{\text{sky}}$ , the number of channels, the sensitivity of each channel  $\sigma_c^{T,E}$  for temperature (T) and E-polarization (E) in  $\mu\text{K}$  and the angular resolution  $\theta_c^{T,E}$  (in arcmin). For Planck HFI, we take the 3 channels with frequencies 100, 143 and 217 GHz, with respectively  $\sigma_{c=1,2,3}^T = 5.4, 6.0, 13.1$  and  $\sigma_{c=2,3}^E = 11.4, 26.7$  and we have  $f_{\text{sky}} = 0.85$  [55]. Since the CVL is an ideal experiment, we put its noise to zero and assume perfect foregrounds removal, so that  $f_{\text{sky}} = 1$ . In order to test the accuracy of our predictions and compare present-day results with the forecasts, we also perform an FMA with WMAP first year parameters, obtaining excellent agreement between the FMA results and the error-bars from actual data. For the purpose of comparison, we include forecasts for the full WMAP 4 years mission, which will also measure E-polarization and reduce present-day errors on the temperature spectrum by a factor of 2. We limit the range of multipoles to  $\ell < 2000$ , because at smaller angular scales non-primary anisotropies begin to dominate (Sunyaev-Zeldovich effect). The authors of ref. [56] discuss the issue of numerical precision of 3 different CMB codes and conclude that they are accurate to within 0.1%. While this is encouraging, it is not of direct relevance to this work, since what matters in the computation of derivatives is not much the absolute precision of the spectra, but rather their relative accuracy.

TABLE I: Cosmological parameters for the fiducial  $\Lambda$ CDM model around which the FMA is performed. We choose a slightly open model to avoid numerical inaccuracies in the derivatives.

|                         |                       |                      |
|-------------------------|-----------------------|----------------------|
| Baryons                 | $\Omega_b$            | 0.046                |
| Matter                  | $\Omega_m$            | 0.270                |
| Dark Energy             | $\Omega_\Lambda$      | 0.720                |
| Radiation               | $\Omega_{\text{rad}}$ | $7.95 \cdot 10^{-3}$ |
| Massless $\nu$ families | $N_\nu$               | 3.04                 |
| Total density           | $\Omega_{\text{tot}}$ | 0.990                |
| Hubble constant         | $h$                   | 0.72                 |
| Optical depth           | $\tau_r$              | 0.166                |
| Spectral index          | $n_s$                 | 0.99                 |
| Normalization           | $A_s$                 | $2 \cdot 10^{-9}$    |

TABLE II: Fisher Matrix forecasts and comparison with present-day results, for different priors and using different combinations of temperature and polarization CMB spectra. Errors are in percent wrt the values of the fiducial model,  $Y_p = 0.24$  and  $\omega_b = 0.0238$  ( 1- $\sigma$  c.l. all other marginalized).

| Temperature, TE-cross, E-polarization |                          |                                    |                          |                                    |                                    |
|---------------------------------------|--------------------------|------------------------------------|--------------------------|------------------------------------|------------------------------------|
|                                       | No priors                |                                    | Flatness                 |                                    | Flatness and $Y_p = 0.24$          |
|                                       | $\frac{\Delta Y_p}{Y_p}$ | $\frac{\Delta \omega_b}{\omega_b}$ | $\frac{\Delta Y_p}{Y_p}$ | $\frac{\Delta \omega_b}{\omega_b}$ | $\frac{\Delta \omega_b}{\omega_b}$ |
| WMAP 4yrs <sup>a</sup>                | ~ 50                     | 2.92                               | ~ 40                     | 2.86                               | 2.86                               |
| Planck                                | 7.60                     | 1.31                               | 4.96                     | 1.26                               | 0.70                               |
| CVL                                   | 2.59                     | 0.34                               | 1.52                     | 0.32                               | 0.13                               |
| Temperature + TE-cross                |                          |                                    |                          |                                    |                                    |
| WMAP 1st yr <sup>b</sup>              | N/A                      | N/A                                | 71.25                    | 5.04                               | 5.04                               |
| WMAP 4yrs <sup>a</sup>                | ~ 75                     | 4.10                               | ~ 60                     | 3.94                               | 3.94                               |
| Planck                                | 8.91                     | 1.74                               | 6.60                     | 1.63                               | 0.74                               |
| CVL                                   | 5.18                     | 0.55                               | 2.84                     | 0.55                               | 0.19                               |

<sup>a</sup> FMA forecast, 4 years mission including E-polarization.

<sup>b</sup> Actual WMAP data and other CMB experiments, this work.

## 3. Forecasts and discussion

Table II summarizes our forecasts for the future measurements and compares them with the results obtained from WMAP actual data.

We notice that when the WMAP full 4 years data will be available (including E-polarization), the error on the baryon density is expected to decrease by a factor of 2 to 2.86%, compared to today’s 5.04% (assuming flatness). Nevertheless, inclusion of  $Y_p$  as a free parameter will still have no effect on the determination of  $\omega_b$  for WMAP, *i.e.*  $Y_p$  will remain an essentially flat direction when marginalized over. While the determination of the helium fraction will improve, the FMA cannot reliably assess quantitatively how much, since for such large er-

rors the likelihood distribution is not Gaussian and the quadratic approximation breaks down. In the table we therefore give the FMA estimation as an indication, with the caveat that the Fisher approximation is likely to be inaccurate for the real errors on  $Y_p$  from WMAP's 4 years data.

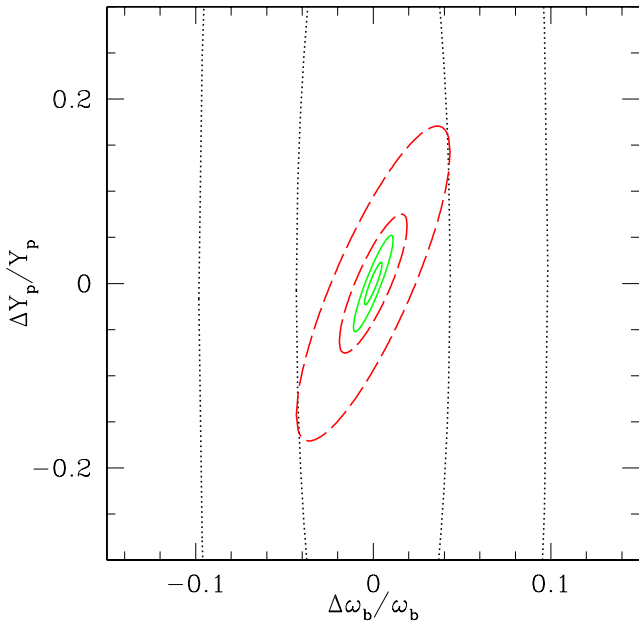


FIG. 8: FMA forecast for the expected errors from WMAP 4 years mission (dotted-black), Planck (dashed-red) and a CVL experiment (solid-green). The ellipses encompass 1- $\sigma$  and 3- $\sigma$  joint confidence regions for  $\omega_b - Y_p$  (all other parameters marginalized). The axis values give the error in wrt the fiducial model values. This forecast is for the full CMB information (Temperature, TE-cross, E-polarization) and assumes flatness.

It is interesting that for Planck the effect of the helium fraction can no longer be neglected. Inclusion of the helium fraction increases the error on  $\omega_b$  by roughly 80%, from 0.70% to 1.26%. The correlation between the two parameters will have to be taken into account, as is evident from Fig. 8. The expected correlation coefficient is  $\text{corr}(Y_p, \omega_b) = 0.84$  (0.91) for Planck (for CVL). The expected 1 -  $\sigma$  error on  $Y_p$  is about 5% for Planck, or  $\Delta Y_p \sim 0.01$ . This is of the same order as the spread in current astrophysical measurements. We conclude that in Planck-accuracy data analysis it will be necessary to include the uncertainty in the determination of the helium mass fraction, at least in the form of a Gaussian

prior over  $Y_p$  of the type we used in the CMB data analysis presented above.

Finally, measuring CMB temperature and polarization with cosmic variance accuracy would allow to constrain  $Y_p$  to within 1.5%, or  $\Delta Y_p \sim 0.0036$  (assuming flatness). Such an ideal measurement would be able to discriminate between the BBN-guided, deuterium based helium value and the current lowest direct helium observations (cf. Fig. 1). We stress once again that at this (or even Planck's) level of precision, a more accurate treatment of the reionization process will be necessary.

#### IV. CONCLUSIONS

We have analysed the ability of CMB observations to determine the helium mass fraction,  $Y_p$ . We find that present data only allow a marginal detection,  $0.160 < Y_p < 0.501$  at 68% c.l.. This determination is completely independent from the usual astrophysical observations and uses CMB data only. We discuss degeneracies between  $Y_p$  and other cosmological parameters, most notably the baryon abundance, the redshift and optical depth of reionization and the spectral index. We conclude that present-day CMB data accuracy does not require the inclusion of  $Y_p$  as a free parameter. We find that Planck will determine the helium mass fraction within 5% (or  $\Delta Y_p \sim 0.01$ ), which however will only allow a marginal discrimination between different astrophysical measurements. Nevertheless, we point out that the uncertainty of the helium fraction will have to be taken into account in order to correctly estimate the errors on the baryon density from Planck. To determine if the emerging baryon tension (from BBN) is related to underestimated systematic error-bars or whether it is an indication of new physics, CMB observation will have to be pushed very close to the cosmic variance limit in both temperature and polarization.

#### Acknowledgement

It is a pleasure to thank Ruth Durrer, Samuel Leach, Anthony Lewis, Christophe Ringeval and Dominik Schwarz for useful discussions. This work was performed on the SUN Enterprise 10000 Supercomputer owned and operated by the University of Geneva. R.T. is partially supported by the Swiss National Science Foundation, the Schmidheiny Fundation and the European Network CMBNET. S.H. thanks the Tomalla foundation for support.

[1] R.H. Cyburt, B.D. Fields and K.A. Olive (2003), astro-ph/0302431

[2] E.W. Kolb, M.S. Turner, “The Early Universe”, Redwood City, USA: Addison-Wesley (1990) 547 p. (Front-

tiers in physics, 69)

[3] D. Kirkman, D. Tytler, N. Suzuki, J.M. O'Meara and D. Lubin, e-Print Archive: astro-ph/0302006

[4] M. Pettini and D.V. Bowen, *Astrophys. J.* **560** (2001) 41 e-print Archive: astro-ph/0104474

[5] Y.I. Izotov and T.X. Thuan, *ApJ* **500** (1998) 188

[6] K.A. Olive, G. Steigman and E.D. Skillman, *ApJ* **483** (1997) 788

[7] A. Peimbert, M. Peimbert and V. Luridiana, *ApJ* **565** (2002) 668

[8] V. Luridiana, A. Peimbert, M. Peimbert and M. Cervino, e-Print Archive: astro-ph/0304152

[9] Y.I. Izotov, F.H. Chaffee, C.B. Foltz, R.F. Green, N.G. Guseva and T. X. Thuan, *ApJ* **527** (1999) 757 e-print Archive: astro-ph/9907228

[10] V. Barger, J. P. Kneller, H. S. Lee, D. Marfatia and G. Steigman, *Phys. Lett. B* **566** (2003) 8

[11] S.G. Ryan, T.C. Beers, K.A. Olive, B.D. Fields, and J.E. Norris, *ApJ* **530** (2000) L57

[12] M. Salaris and A. Weiss, e-Print Archive: astro-ph/0104406

[13] S. Burles, K.M. Nollett and M.S. Turner, *ApJ* **552** (2001) L1 e-print Archive: astro-ph/0010171

[14] S.H. Hansen, G. Mangano, A. Melchiorri, G. Miele and O. Pisanti, *Phys. Rev. D* **65**, 023511 (2002) e-print Archive: astro-ph/0105385

[15] R.E. Lopez and M.S. Turner, *Phys. Rev. D* **59** (1999) 103502 e-print Archive: astro-ph/9807279

[16] S. Esposito, G. Mangano, G. Miele and O. Pisanti, *Nucl. Phys. B* **568** (2000) 421

[17] S. Esposito, G. Mangano, G. Miele and O. Pisanti, *JHEP* **09** (2000) 038

[18] A.D. Dolgov, S.H. Hansen, S. Pastor and D.V. Semikoz, *Nucl. Phys. B* **548** (1999) 385 e-print Archive: hep-ph/9809598

[19] A.D. Dolgov, S.H. Hansen, G. Raffelt and D.V. Semikoz, *Nucl. Phys. B* **590** (2000) 562 e-print Archive: hep-ph/0008138

[20] P. Di Bari and R. Foot, *Phys. Rev. D* **63** (2001) 043008 e-print Archive: hep-ph/0008258

[21] D. P. Kirilova, *Astropart. Phys.* **19** (2003) 409 e-print Archive: astro-ph/0109105

[22] X.D. Shi, G.M. Fuller and K. Abazajian, *Phys. Rev. D* **60** (1999) 063002 e-print Archive: astro-ph/9905259

[23] P. Crotty, J. Lesgourgues and S. Pastor, *Phys. Rev. D* **67** (2003) 123005 E. Pierpaoli, e-Print Archive: astro-ph/0302465; S. Hannestad, e-Print Archive: astro-ph/0303076; P. Di Bari, e-Print Archive: astro-ph/0302433; S. Pastor, arXiv:hep-ph/0306233

[24] H. S. Kang and G. Steigman, *Nucl. Phys. B* **372** (1992) 494; J. Lesgourgues and S. Pastor, *Phys. Rev. D* **60** (1999) 103521

[25] A.D. Dolgov et al., *Nucl. Phys. B* **632** (2002) 363; Y.Y. Wong, *Phys. Rev. D* **66** (2002) 025015; K.N. Abazajian, J.F. Beacom and N.F. Bell, *Phys. Rev. D* **66** (2002) 013008

[26] V. Barger, J. P. Kneller, P. Langacker, D. Marfatia and G. Steigman, arXiv:hep-ph/0306061.

[27] D.N. Spergel *et al.*, e-Print Archive: astro-ph/0302209

[28] Iu.E. Liubarskii and R.A. Sunyaev, *Astron. Astrophys.* **123** (1983) 171

[29] W. Hu, D. Scott, N. Sugiyama and M.J. White, *Phys. Rev. D* **52** (1995) 5498, e-print Archive: astro-ph/9505043

[30] S. Seager, D.D. Sasselov and D. Scott, *Astrophys. J. Supp.* **128** (2000) 407, e-print Archive: astro-ph/9912182

[31] S. Seager, D.D. Sasselov and D. Scott, *Astrophys. J.* **523** (1999) L1, e-print Archive: astro-ph/9909275

[32] Z. Haiman, to appear in Carnegie Observatories Astrophysics Series, Vol. 1, ed. L. C. Ho (Cambridge: Cambridge Univ. Press), astro-ph/0304131

[33] R. H. Becker *et al.* *AJ* **122** (2001) 2850; X. Fan *et al.* *Astron. J.*, **123** (2002) 1247

[34] R. Cen, arXiv:astro-ph/0210473; L. Hui and Z. Haiman, arXiv:astro-ph/0302439.

[35] T. Theuns *et al.*, *Astrophys.J.* 574 (2002) L111-L114 e-print Archive: astro-ph/0206319

[36] <http://cosmologist.info/cosmomc/>

[37] A. Lewis and S. Bridle, *Phys. Rev. D* **66**, 103511 (2002)

[38] A. Kogut *et al.*, e-Print Archive: astro-ph/0302213

[39] G. Hinshaw *et al.* (2003), e-Print Archive: astro-ph/0302222

[40] L. Verde *et al.* (2003), e-Print Archive: astro-ph/0302218

[41] T. Pearson *et al.* (2002), e-Print Archive: astro-ph/0205388

[42] <http://cosmologist.info/ACBAR>

[43] C.L. Kuo *et al.* (2003), e-Print Archive: astro-ph/0212289

[44] A. Gelman and D. Rubin, *Statistical Science*, **7** (1992) 457

[45] L. Knox, *Phys. Rev. D* **52** (1995) 4307

[46] G. Efstathiou and J.R. Bond *MNRAS* **304** (1999) 75

[47] R.J. Bond, G. Efstathiou and M. Tegmark, *Mon. Not. Roy. Astron. Soc.* **291** (1997) L33 e-print Archive: astro-ph/9702100

[48] R. Bowen, S.H. Hansen, A. Melchiorri, J. Silk and R. Trotta, *Mon. Not. Roy. Astron. Soc.* **334** (2002) 760 e-print Archive: astro-ph/0110636

[49] C. J. Martins, A. Melchiorri, R. Trotta, R. Bean, G. Rocha, P. P. Avelino and P. T. Viana, *Phys. Rev. D* **66** (2002) 023505 [arXiv:astro-ph/0203149].

[50] C. J. Martins, A. Melchiorri, G. Rocha, R. Trotta, P. P. Avelino and P. Viana, arXiv:astro-ph/0302295.

[51] M. Zaldarriaga and U. Seljak, *Phys. Rev. D* **55**, 1830-1840 (1997) e-print Archive: astro-ph/9609170.

[52] M. Tegmark, A.N. Taylor and A.F. Heavens, e-Print Archive: astro-ph/9603021

[53] A. Kosowsky, M. Milosavljevic and R. Jimenez, *Phys. Rev. D* **66** (2002) 063007 e-print Archive: astro-ph/0206014

[54] R. Durrer, *J. Phys. Stud.* **5** (2001) 177 e-print Archive: astro-ph/0109522

[55] Planck Homepage, <http://astro.estec.esa.nl/Planck> (2003)

[56] U. Seljak, N. Sugiyama, M. White, M. Zaldarriaga, e-Print Archive: astro-ph/0306052